

## Charge density excitations of two-dimensional magnetoplasma in semiconductor superlattices

Manvir S. Kushwaha

Citation: [Journal of Applied Physics](#) **73**, 792 (1993); doi: 10.1063/1.353340

View online: <http://dx.doi.org/10.1063/1.353340>

View Table of Contents: <http://scitation.aip.org/content/aip/journal/jap/73/2?ver=pdfcov>

Published by the [AIP Publishing](#)

---

### Articles you may be interested in

[Two-dimensional magnetic interactions and magnetism of high-density charges in a polymer transistor](#)  
Appl. Phys. Lett. **102**, 133301 (2013); 10.1063/1.4800550


[Shocks, explosions, and vortices in two-dimensional homogeneous quantum magnetoplasma](#)  
Phys. Plasmas **18**, 022303 (2011); 10.1063/1.3551577

[Parametric studies of nonlinear magnetosonic waves in two-dimensional quantum magnetoplasmas](#)  
Phys. Plasmas **16**, 022301 (2009); 10.1063/1.3073669

[Erratum: "Charge density excitations in semiconductor superlattices" \[J. Appl. Phys. 6 2, 1895 \(1987\)\]](#)  
J. Appl. Phys. **65**, 3303 (1989); 10.1063/1.343436

[Charge density excitations in semiconductor superlattices](#)  
J. Appl. Phys. **62**, 1895 (1987); 10.1063/1.339577

---

**SHIMADZU**  
Excellence in Science

**Powerful, Multi-functional UV-Vis-NIR and FTIR Spectrophotometers**

Providing the utmost in sensitivity, accuracy and resolution for applications in materials characterization and nano research

- Photovoltaics
- Polymers
- Thin films
- Paints
- Ceramics
- DNA film structures
- Coatings
- Packaging materials

[Click here to learn more](#)

A row of four Shimadzu spectrophotometers is shown. From left to right: a small desktop unit, a larger desktop unit with a sample holder, a large floor-standing unit with a control panel, and a tall, narrow floor-standing unit.

# Charge density excitations of two-dimensional magnetoplasma in semiconductor superlattices

Manvir S. Kushwaha<sup>a)</sup>

*Laboratoire de Physique du Solide, Faculté des Sciences et Techniques, Université de Haute Alsace, 4, rue des Frères Lumière, 68093 Mulhouse Cédex, France*

(Received 14 May 1992; accepted for publication 18 September 1992)

This paper presents the theoretical investigation of collective charge density excitations in two-dimensional semiconductor superlattices subjected to a perpendicular magnetic field. We use a simple electromagnetic theory with a two-dimensional Dirac- $\delta$  function for the charge density profile. The magnetoplasmon dispersion relations are derived for an infinite and semi-infinite superlattices, both type II (InAs-GaSb systems) and type I (GaAs-Al<sub>x</sub>Ga<sub>1-x</sub>As systems). We emphasize on the magnetoplasma polaritons of semi-infinite superlattices. A detailed analytical diagnosis has been made of the dispersion relations to study the various limiting situations. The surface charge density excitations in the type II superlattices display a broken degeneracy in the retarded limit due to the presence of an applied magnetic field. This interestingly happens with the surface plasmon branch lying within the gap between two bulk bands. Moreover, the  $Q$  (Bloch wave vector) = 0 edge of the bulk bands exhibits the splitting of the dispersion curve at a frequency ( $\omega$ ) greater than the cyclotron frequency ( $\omega_c$ ). Application of a magnetic field results, in general, in pushing the whole spectrum lying above  $\omega = \omega_c$ . The numerical results, including the retardation effects, both for zero and nonzero magnetic fields, have been presented for several illustrative cases.

## I. INTRODUCTION

Over the past seven or eight years, there have been a number of significant advances in solid state electronics which can be attributed to a unique combination of basic concepts, perfection of new materials, and the developments of new device principles. The synthesis of semiconductor heterostructures with specified band gap has led to the discovery of totally unexpected two-dimensional (2D) behavior of charge carriers. Because of their applications to novel and potentially useful devices, the physics of semiconductor heterostructures and superlattices has attracted a great deal of attention, both experimental and theoretical, in recent years.<sup>1</sup> Theoretically, the reduced degrees of freedom allow detailed and often exact calculations. Experimentally new and unexpected phenomena have been observed. Initial investigations have been made of various elementary collective excitations which are of paramount importance to a complete understanding of these tailor-made semiconductors. Studies of such elementary collective excitations were stimulated by a first, detailed and pertinent paper by Das Sarma and Quinn.<sup>2</sup> Since then a number of authors have devoted to the understanding of various types of collective excitations in these 2D systems.<sup>3-13</sup>

There are two types of compositional superlattices which have been extensively studied in the recent past. One of these (referred to as type I) is typified by a GaAs-Al<sub>x</sub>Ga<sub>1-x</sub>As system. The simplest model of type I superlattice which will be concerned with is a low temperature periodic system of 2D electron gas. The other type of su-

perlattice system (referred to as type II) is typified by an InAs-GaSb system. For our purpose it is sufficient to consider type II superlattice as a periodic arrangement of two dimensionally confined alternating electron and hole layers. For conceptual details of the physics of the superlattice systems considered here, see Refs. 2, 7, and 14.

A two-dimensional electronic system, such as can be realized in the aforesaid semiconductor superlattices, consists of charge carriers which are mobile in the plane along the interfaces and confined in the perpendicular direction (i.e., along the superlattice axis). This confinement leads to the formation of discrete subbands. Application of an external magnetic field along the superlattice axis splits each subband into Landau levels and leads therefore to a completely quantized system. The case where the magnetic field is oriented in the same direction as the confining electric field is however a very special one because only then the Hamiltonian can be separated in electric part leading the subbands and a magnetic part leading to Landau levels. For any other orientation this separation is not possible anymore and the band structure in the presence of a magnetic field is much more complicated. The effect of an applied magnetic on a 2D electronic system is very striking and easily observable. Investigations of such effects on 2D systems have led to discover an unexpected potentially new physics. The discovery of quantum Hall effects, both integral and fractional, is a live example.

The effect of an external magnetic field on the collective (bulk) excitations in the superlattice systems was studied fairly completely by Quinn and co-workers.<sup>6,7</sup> They used the linear response theory to calculate the density response of the system to an external perturbation. Their self-consistent field method (SCFM) accommodates both intra and intersubband modes on equal footing and in-

<sup>a)</sup>Permanent address: Instituto de Física, Universidad Autónoma de Puebla, Apdo. Post. J-48, Puebla-72570, Mexico.

cludes many-body effects such as resonant screening and Vertex corrections, leading to depolarization and excitonic shifts. It is, however, worthwhile discussing how a rigorous technique like SCFM which produces complicated analytical results was forced to achieve simple and readily conclusive results that can be obtained in the framework of a relatively simple electromagnetic theory.

The SCFM is, in fact, a dielectric formulation of a many-electron system which involves a nonlocal dielectric function  $\epsilon(q, \omega)$  to give a complete description of the optical properties of a superlattice, as for any other solid. As it is well known, the dispersion relation of the collective excitations is given by the zeros of  $\epsilon(q, \omega)$ . In the SCFM followed by Quinn and co-workers,<sup>7</sup> the authors derived the linear response of the superlattice systems to an external perturbation ( $V_{ex}$ ). The dispersion relation for collective modes is obtained finally by imposing the condition of self-sustaining plasma oscillations (i.e.,  $V_{ex}=0$ ). The authors proceed assuming the minibands as flat and invoke the Hartree approximation in which the total Hamiltonian is replaced by its noninteracting part. The former approximation leads to neglect of the overlap of envelope wave functions between adjacent layers and the latter to the construction of random phase approximation. In order to obtain the intrasubband modes, the ones we investigate here, the authors have further resorted to a number of simplifying assumptions. For instance, they set  $n=0=m$ ,  $n$  and  $m$  being the subband indexes, use the long wavelength limit and omit the vertex corrections. Note that the first of these assumptions reduces their envelope wave function to a purely 2D delta function for charge density profile, just as employed in the present work. In view of this, the SCFM of Quinn and co-workers effectively reduces to a semiclassical approach followed by the present author and produces identical analytical results which allow an easy access of interesting special cases: namely, the strong and weak coupling between adjacent layers.

In this paper we examine the electronic collective modes, both bulk and surface, which occur in these systems. We carry this out in the framework of a simple electromagnetic theory where the confinement of the charge carriers to the 2D planes is governed by the Dirac-delta function. We are interested in the situation where the width of the potential well or barriers in the superlattice structure are much larger than de-Broglie wavelength so that the quantum size effects are unimportant. It is noteworthy that the simpler technique used here provides us with the exact analogs of the dispersion relations for collective (bulk) excitations, for both types of superlattice systems, derived by Quinn and co-workers using a somewhat more complicated method. The new results for magnetoplasma polaritons of the truncated superlattices have been examined by subjecting them to various special limits. It can readily be seen that our general dispersion relations for these limits reproduces exactly the proper results previously reported in the literature.

The rest of the paper is organized as follows. In Sec. II, we derive the general dispersion relations for bulk and surface magnetoplasmons for type II superlattice systems.

Section III is devoted to present the similar analytic results for type I superlattice systems. The numerical examples are discussed in Sec. IV. We conclude in Sec. V, summarizing our findings and pointing out some possible future improvements of our theory.

## II. TYPE II SUPERLATTICES

We consider a periodic array of 2D layers: alternate layers contain electrons (with density  $n_e$  per unit area and effective mass  $m_e$ ) and holes (with density  $n_h$  per unit area and effective mass  $m_h$ ). The superlattice structure consists of equally spaced, parallel 2D planes centered at  $z=0, d, 2d, \dots, ld$ , where  $l$  is the layer index and  $d$  the spacing between electron and hole layers. Thus periodicity of the system lies along the superlattice axis (taken to be the  $z$  axis of the cartesian coordinate system). The even ( $l=0, 2, 4$ , etc.) and odd ( $l=1, 3, 5$ , etc.) numbered layers are assumed to be occupied by 2D electron gas (2DEG) and 2D hole gas (2DHG), respectively. The external magnetic field ( $B_0$ ) is oriented along the superlattice axis. Further we assume that the motion of the charge carriers is free in 2D  $x$ - $y$  plane and the superlattice potential confines the charge carriers to the planes  $z=ld$ . The tunneling of the carriers between the consecutive layers is completely forbidden. This model of periodic 2D multilayers located at  $z=ld$  is assumed to be embedded in a background characterized by dielectric constant  $\epsilon_s$  and filling the space  $z \geq 0$ .

### A. Infinite superlattice

First we consider an infinite superlattice system. To obtain the dispersion relation for collective charge density excitations we resort to the standard electromagnetic theory using the Maxwell equations and the boundary conditions. After eliminating the magnetic field variable, we write the following wave field equation in terms of the macroscopic electric field

$$\nabla \times (\nabla \times \mathbf{E}) - q_0^2 \epsilon_s \mathbf{E} = i \frac{4\pi}{\omega} q_0^2 \left( \sum_l \mathbf{J}_e \delta(z - 2ld) + \sum_l \mathbf{J}_h \delta[z - (2l+1)d] \right), \quad (1)$$

where  $q_0 = \omega/c$  ( $\omega$  and  $c$  being, respectively, the angular frequency and velocity of light in vacuum) is the vacuum wave vector.  $\mathbf{J}_e$  and  $\mathbf{J}_h$  are, respectively, the electron and the hole surface current densities. The charge density profiles along the superlattice axis have been represented by Dirac delta functions. This leads us to infer that the surface current densities are nonzero only at the planes  $z=ld$ . Note that the superlattice period is  $2d$ . The spatial and temporal dependence of the fields is taken of the form of  $\sim e^{i(\mathbf{q} \cdot \mathbf{r} - \omega t)}$ .

The determination of the dispersion relation requires the matching of certain electromagnetic boundary conditions at the interfaces specifying two different constituent layers:  $2ld < z < (2l+1)d$  (specified as region A) and  $(2l+1)d < z < 2(l+1)d$  (specified as region B). The standard boundary conditions we shall use for the present system are

$$(\mathbf{E}_1 - \mathbf{E}_2) \times \hat{n} = 0, \quad (2)$$

$$(\mathbf{H}_1 - \mathbf{H}_2) \times \hat{n} = \frac{4\pi}{c} \mathbf{J}_s, \quad (3)$$

where the subscript  $s (\equiv e, h)$  stands for an electron or hole, and  $\hat{n}$  is the normal unit vector directed from medium 1 to medium 2. The surface current density ( $\mathbf{J}$ ) is related to the conductivity tensor ( $\tilde{\sigma}$ ) and the polarizability tensor ( $\tilde{\chi}$ ) by the relation

$$\mathbf{J} = \tilde{\sigma} \cdot \mathbf{E} = -i\omega \tilde{\chi} \cdot \mathbf{E}. \quad (4)$$

We write the field distributions in the two above-mentioned regions in the form

$$\mathbf{E}(\mathbf{r}, t) = \mathbf{E}(z) e^{i(qy - \omega t)}, \quad (5)$$

where  $\mathbf{E}(z)$  for region  $i (\equiv e, h)$  is expressed as

$$\mathbf{E}^i(z) = \mathbf{E}_1^i e^{\alpha z} + \mathbf{E}_2^i e^{-\alpha z}. \quad (6)$$

Analogous solutions can be written for the magnetic field variable ( $\mathbf{B} \equiv \mathbf{H}$ ). Here  $\alpha = (q^2 - q_0^2 \epsilon_s)^{1/2}$ ,  $q$  being the wave vector in the plane assumed to be parallel to the  $\hat{y}$  axis with no loss of generality. The periodicity of the superlattice system is accounted for by making the field solutions  $\mathbf{E}(z)$  to satisfy the Bloch theorem. To meet this requirement, we write

$$\mathbf{E}_l(z) = e^{2ikd} \mathbf{E}_{l-1}(z), \quad (7)$$

where  $k (\equiv q_z)$  is the normal component of wave vector along the superlattice axis. The use of Eqs. (2)–(7) leads us to match the standard electromagnetic boundary conditions at the two appropriate interfaces [i.e.,  $z = (2l+1)d$  and  $z = 2ld$ ] of the periodic system. Imposing the condition of nontrivial solutions results to give

$$\begin{aligned} & \left[ \chi_{yy}^e \chi_{yy}^h (s_1^2 - s_2^2) + \frac{\epsilon_s}{2\pi\alpha} (\chi_{yy}^e + \chi_{yy}^h) s_1 + \left( \frac{\epsilon_s}{2\pi\alpha} \right)^2 \right] \left[ \chi_{xx}^e \chi_{xx}^h (s_1^2 - s_2^2) - \frac{\alpha}{2\pi q_0^2} (\chi_{xx}^e + \chi_{xx}^h) s_1 + \left( \frac{\alpha}{2\pi q_0^2} \right)^2 \right] \\ & + \left( \chi_{yy}^e (s_1^2 - s_2^2) + \frac{\epsilon_s}{2\pi\alpha} s_1 \right) \left( \chi_{xx}^e (s_1^2 - s_2^2) - \frac{\alpha}{2\pi q_0^2} s_1 \right) (\chi_{xy}^h)^2 + \left( \chi_{yy}^h (s_1^2 - s_2^2) + \frac{\epsilon_s}{2\pi\alpha} s_1 \right) \left( \chi_{xx}^h (s_1^2 - s_2^2) \right. \\ & \left. - \frac{\alpha}{2\pi q_0^2} s_1 \right) (\chi_{xy}^e)^2 + (\chi_{xy}^e)^2 (\chi_{xy}^h)^2 (s_1^2 - s_2^2)^2 - \frac{\epsilon_s}{2\pi^2 q_0^2} \chi_{xy}^e \chi_{xy}^h s_1^2 = 0, \end{aligned} \quad (8)$$

where  $s_1$  and  $s_2$  are the structure factors defined by

$$\begin{aligned} s_1 &= \frac{\sinh(2\alpha d)}{\cosh(2\alpha d) - \cos(2kd)} \\ s_2 &= \frac{2\sinh(\alpha d) \cos(kd)}{\cosh(2\alpha d) - \cos(2kd)}, \end{aligned} \quad (9)$$

and  $\chi_{ij}$ 's are the elements of the 2D polarizability tensor ( $\tilde{\chi}$ ), given by

$$\begin{aligned} \chi_{yy}^{(i)} &= \chi_{xx}^{(i)} = \frac{n_i e^2}{m_i} \frac{1}{(\omega_{ci}^2 - \omega^2)} \\ \chi_{xy}^{(i)} &= -\chi_{yx}^{(i)} = -i \frac{n_i e^2}{m_i} \frac{\omega_{ci}}{\omega(\omega_{ci}^2 - \omega^2)}, \end{aligned} \quad (10)$$

where  $m_i$  is the effective mass of the electron ( $i \equiv e$ ) or the hole ( $i \equiv h$ ), and  $\omega_{ci} (= e_i B_0 / m_i c)$  is the electron ( $i \equiv e$ ) or hole ( $i \equiv h$ ) cyclotron frequency. Equation (8) is the dispersion relation of 2D magnetoplasmons in the type II superlattice system. It can be readily seen that this is exactly identical to Eq. (32) of Tselis and Quinn.<sup>6</sup> We will analyze some limiting cases of Eq. (8) a little further on.

## B. Semi-infinite superlattice

We now consider a physically important case when the infinite periodic superlattice, described in the preceding subsection, is truncated at an interfaces  $z=0$  such that the region  $-\infty < z \leq 0$  is occupied by an insulating (or, dielectric) medium characterized by dielectric constant  $\epsilon_0$ . In

order to derive the general dispersion relation of 2D magnetoplasma polaritons we follow exactly the same prescription of writing down the boundary conditions at the appropriate interfaces inside as well as at the terminating plane  $z=0$ . However, in this case we are interested in the situation in which the fields in the region  $z > 0$  satisfy the relation

$$\mathbf{E}_l(z) = e^{-2\beta d} \mathbf{E}_{l-1}(z), \quad (11)$$

instead of the Bloch condition stated in Eq. (7), where  $\beta = -ik$ . Note that Eq. (8) still holds good if the structure factors, in Eqs. (9), are modified by replacing  $\cos(nkd)$  by  $\cosh(n\beta d)$ ;  $n \equiv 1, 2$ . The boundary conditions at  $z=0$  are formally identical to those at  $z=2ld$ , with  $l=0$ , except that there is an abrupt change in the background dielectric constant from  $\epsilon_s$  to  $\epsilon_0$ . The resulting dispersion relation for surface excitations is

$$(\alpha_1 \beta_2 - \alpha_2 \beta_1) (\beta_1 \gamma_2 - \beta_2 \gamma_1) - (\alpha_1 \gamma_2 - \alpha_2 \gamma_1)^2 = 0, \quad (12)$$

where

$$\alpha_1 = \text{cosech}^4(\alpha d) \quad (13a)$$

$$\begin{aligned} \beta_1 &= \text{cosech}^2(\alpha d) \{ [\delta_1 \coth(\alpha d) + \delta_3] + [\delta_2 \coth(\alpha d) \\ &+ \delta_4] + M_{xy}^C \}, \end{aligned} \quad (13b)$$

$$\begin{aligned}\gamma_1 &= [(\delta_1 \coth(\alpha d) + \delta_3)(\delta_2 \coth(\alpha d) + \delta_4) + M_{xy}^A \delta_5 \delta_6 \\ &\quad + M_{xy}^B \delta_1 \delta_2 + M_{xy}^A M_{xy}^B + M_{xy}^C \operatorname{cosech}^2(\delta d)], \quad (13c) \\ \alpha_2 &= [\coth(\alpha d) - \lambda][\coth(\alpha d) - \mu], \quad (13d) \\ \beta_2 &= \delta_1 [\coth(\alpha d) - \mu] + \delta_2 [\coth(\alpha d) - \lambda], \quad (13e) \\ \gamma_2 &= \delta_1 \delta_2 + M_{xy}^A, \quad (13f)\end{aligned}$$

and

$$\delta_1 = \coth(\alpha d) + (D_1 + \lambda), \quad D_1 = 4\pi\alpha\chi_{yy}^e/\epsilon_s, \quad (14a)$$

$$\delta_2 = \coth(\alpha d) - (D_2 - \mu), \quad D_2 = 4\pi q_0^2 \chi_{xx}^e/\alpha, \quad (14b)$$

$$\delta_3 = 1 + C_1 \delta_1 + (D_1 + \lambda) \coth(\alpha d), \quad C_1 = 4\pi\alpha\chi_{yy}^h/\epsilon_s, \quad (14c)$$

$$\delta_4 = 1 - C_2 \delta_2 - (D_2 - \mu) \coth(\alpha d), \quad C_2 = 4\pi q_0^2 \chi_{xx}^h/\alpha, \quad (14d)$$

$$\delta_5 = 2 \coth(\alpha d) + C_1, \quad (14e)$$

$$\delta_6 = 2 \coth(\alpha d) - C_2, \quad (14f)$$

$$M_{xy}^A = \frac{4\pi q_0^2}{\alpha} \times \frac{4\pi\alpha}{\epsilon_s} \chi_{xy}^e \chi_{yx}^e, \quad (14g)$$

$$M_{xy}^B = \frac{4\pi q_0^2}{\alpha} \times \frac{4\pi\alpha}{\epsilon_s} \chi_{xy}^h \chi_{yx}^h, \quad (14h)$$

$$M_{xy}^C = \frac{4\pi q_0^2}{\alpha} \times \frac{4\pi\alpha}{\epsilon_s} (\chi_{xy}^e \chi_{yx}^h + \chi_{yx}^e \chi_{xy}^h), \quad (14i)$$

$$\lambda = \epsilon_0 \alpha / \epsilon_s \alpha_0, \quad \mu = \alpha_0 / \alpha, \quad \alpha_0 = (q_y^2 - q_0^2 \epsilon_0)^{1/2}. \quad (14j)$$

### III. TYPE I SUPERLATTICES

In this section we proceed to discuss the collective charge density excitations in the type I superlattice system. The model we use for the electronic structure of this system is essentially the same as that considered for the type II superlattice system, except that every other layer contains electrons instead of holes. In other words, a type I superlattice is assumed to be made up of a periodic array of 2DEG layers embedded in a material characterized by a background dielectric constant  $\epsilon_s$ . Clearly, then, the period of the superlattice will be half of that of type II superlattice. Again, we assume that the charge carriers are two-dimensionally confined with no overlap of carrier wave functions between adjacent layers. This is expected to be a physically good approximation for low electron densities when only the lowest 2D subband in each quantum well is occupied.

The model of the type I superlattice, as described above, leads one to infer that the generalization of the analytical results obtained in the case of the type II superlattice to those of type I is quite straightforward. There is, in fact, no need to expand on simply rewriting the whole formalism as described in subsections II A and II B. We will, therefore, be quite succinct in this section, essentially quoting the important results instead of going through the

details. The keystone to obtain directly the dispersion relations for type I superlattice is to substitute  $\chi_{ij}^h = 0$  and replace  $2d$  by  $d$  in the corresponding results of the type II superlattice.

#### A. Infinite superlattice

Substituting  $\chi_{ij}^h (i, j = x, y) = 0$  and replacing  $2d$  by  $d$  in Eq. (8) yields

$$\left(S\chi_{yy}^e + \frac{\epsilon_s}{2\pi\alpha}\right)\left(S\chi_{xx}^e - \frac{\alpha}{2\pi q_0^2}\right) - (S\chi_{xy}^e)(S\chi_{yx}^e) = 0, \quad (15)$$

where  $\chi_{ij}^e$  are as defined in Eqs. (10) and

$$S = \frac{\sinh(\alpha d)}{\cosh(\alpha d) - \cos(kd)}, \quad (16)$$

is the structure factor. Equation (15) is an exact analog of Eq. (23) of Tselis and Quinn.<sup>6</sup> It is readily seen that the effect of the multilayer structure is to modify the polarizability tensor by the structure factor  $S$ . Equation (15) is the dispersion relation for collective (bulk) 2D magnetoplasmons propagating in the type I superlattice.

#### B. Semi-infinite superlattice

We now consider the infinite superlattice system truncated at an interface  $z=0$  such that the region  $-\infty < z \leq 0$  is assumed to be occupied by an insulating material characterized by a dielectric constant  $\epsilon_0$ . As discussed above, we can immediately write down the dispersion relation for the 2D magnetoplasmon polaritons in the type I superlattice, just by substituting  $\chi_{ij}^h = 0$  and replacing  $2d$  by  $d$  in Eq. (12). The result is

$$(\alpha'_1 \beta'_2 - \alpha'_2 \beta'_1)(\beta'_1 \gamma'_2 - \beta'_2 \gamma'_1) - (\alpha'_1 \gamma'_2 - \alpha'_2 \gamma'_1)^2 = 0, \quad (17)$$

where

$$\alpha'_1 = \operatorname{cosech}^4(\alpha d/2) \quad (18a)$$

$$\begin{aligned}\beta'_1 &= \operatorname{cosech}^2(\alpha d/2) \{ [\delta'_1 \coth(\alpha d/2) + \delta'_3] \\ &\quad + [\delta'_2 \coth(\alpha d/2) + \delta'_4] \}, \quad (18b)\end{aligned}$$

$$\begin{aligned}\gamma'_1 &= \{ [\delta'_1 \coth(\alpha d/2) + \delta'_3] [\delta'_2 \coth(\alpha d/2) + \delta'_4] \\ &\quad + M_{xy}^A \delta'_5 \delta'_6 \}, \quad (18c)\end{aligned}$$

$$\alpha'_2 = [\coth(\alpha d/2) - \mu][\coth(\alpha d/2) - \lambda], \quad (18d)$$

$$\beta'_2 = \delta'_1 [\coth(\alpha d/2) - \mu] + \delta'_2 [\coth(\alpha d/2) - \lambda], \quad (18e)$$

$$\gamma'_2 = \delta'_1 \delta'_2 + M_{xy}^A, \quad (18f)$$

and

$$\delta'_1 = \coth(\alpha d/2) + (D_1 + \lambda), \quad (19a)$$

$$\delta'_2 = \coth(\alpha d/2) - (D_2 - \mu), \quad (19b)$$

$$\delta'_3 = 1 + (D_1 + \lambda) \coth(\alpha d/2), \quad (19c)$$

$$\delta'_4 = 1 - (D_2 - \mu) \coth(\alpha d/2), \quad (19d)$$

$$\delta'_5 = 2 \coth(\alpha d/2), \quad (19e)$$

$$\delta'_6 = \delta'_7. \quad (19f)$$

We have made an extensive analytical diagnosis of the dispersion relations [Eqs. (8), (12), (15), and (17)] by subjecting them to various special limits, viz.  $B_0=0$ , weak coupling limit ( $\alpha d \gg 1$ ), strong coupling limit ( $\alpha d \ll 1$ ), and nonretarded limit ( $c \rightarrow \infty$ ). It is found that within these

special limits our general dispersion relations reproduce exactly the previously reported well established results both in the absence<sup>2,4,10</sup> and in the presence<sup>2,5-7</sup> of an applied magnetic field.

It is worthwhile mentioning that Eqs. (12) and (17) are the important new results of this paper for type II and type I superlattice systems, respectively. In what follows, we discuss the numerical results based on Eqs. (8) and (12) for type II and Eqs. (15) and (17) for type I superlattice systems. For this purpose we use the following values of the parameters

$$\text{Type I: } \epsilon_s = 13.0; \quad n_e = 7.34 \times 10^{11} \text{ cm}^{-2}; \quad m_e = 0.0665 m_0; \\ d = 600 \text{ \AA}; \quad \omega_{ce}/\Omega_{pe} = 0.5, 0.9; \quad \epsilon_0 = 1.0$$

$$\text{Type II: } \epsilon_s = 13.0; \quad n_e = n_h = 4.2 \times 10^{11} \text{ cm}^{-2}; \quad m_e = 2.0 m_h = 0.0665 m_0; \\ d = 550 \text{ \AA}; \quad \omega_{ce}/\Omega_{pe} = 0.5, 0.9; \quad \omega_{ch}/\Omega_{pe} = -(m_e/m_h) \times (\omega_{ce}/\Omega_{pe}).$$

Here  $\Omega_{pi} = [4\pi n_i e^2 / m_i (2d)]^{1/2}$  is the three-dimensional (3D) unscreened plasma frequency.

#### IV. NUMERICAL RESULTS

In presenting the numerical results it is convenient to introduce the dimensionless wave vector  $\zeta = qd$  and dimensionless frequency  $\xi = \omega/\Omega_{pe} \times \Omega_{pe}d/c = \omega d/c$ . Since we are interested to investigate the effect of an applied magnetic field on the 2D plasmons, two representative values of  $B_0$ , as mentioned in the preceding section, are considered. In order to provide a comparison, we present results both with and without an applied magnetic field. In spite of the mathematical complexity, we have presented some analyt-

ical diagnosis in order to substantiate a number of critical starting points attained by the bulk band edges.

##### A. Type I superlattice

Figure 1 depicts the plot of  $\xi$  versus  $kd$  for  $B_0=0$ . The effect of the multilayer system in the broadening of a single 2DEG layer plasmon into a band is evident. The bandwidth is determined by the properties of the superlattice as discussed by Bloss and Brody.<sup>3</sup> The complete dispersion relations of bulk and surface plasmons in the absence of an applied magnetic field<sup>10</sup> are plotted in Fig. 2. The shaded region shows the bulk plasmon band continuum whose boundaries correspond to  $k=0$  and  $k=\pi/d$ . For small values of  $\xi$ , corresponding to the strong coupling limit, the mode, for  $k=0$ , starts at an effective 3D plasma frequency  $\omega = \Omega_{pe}/\sqrt{\epsilon_s}$  which means  $\xi \simeq 0.004244$ , whereas that for  $k=\pi/d$  starts with linear dispersion at  $\xi=0$ . The solid line above the upper edge of the bulk band is the surface plasmon polariton whose existence is in analogy with the criteria as discussed by Giuliani and Quinn<sup>4</sup> and Kushwaha.<sup>10</sup> The intersection of the polariton mode with the band edge occurs at a critical value of  $q=q^*$  given by

$$\alpha d = \ln \left| \frac{1+\lambda}{1-\lambda} \right|. \quad (20)$$

Equation (20), in the nonretarded limit ( $c \rightarrow \infty$ ), reduces to Eq. (3) of Giuliani and Quinn.<sup>4</sup> For  $q < q^*$  the polariton modes do not exist because the decay constant  $\alpha$  is purely imaginary. It is found that the value of  $q^*$  decreases when the retardation effect is included. This leads us to believe that the attenuated total reflection (ATR) seems an appropriate method for observing these surface polaritons. In the nonretarded limit the situation takes a different turn and ATR has been argued to be an unlikely method of observation of these modes.<sup>4,10</sup>

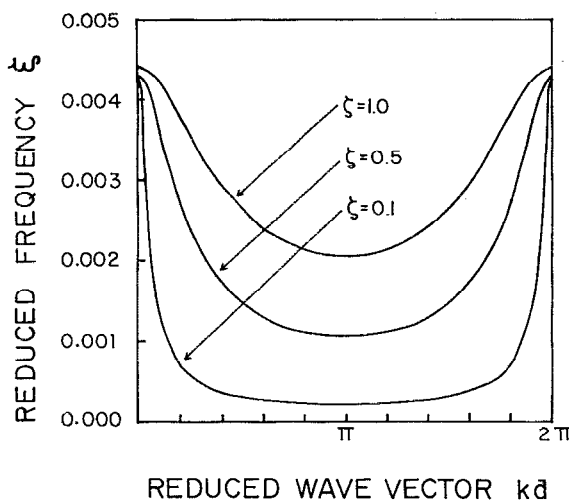


FIG. 1. Plasmon dispersion relation of type I superlattice plotted as  $\xi$  vs  $kd$ , for  $\zeta=0.1, 0.5$ , and  $1.0$ , in the absence of an applied magnetic field. The parameters used are:  $\epsilon_s = 13.0$ ;  $n_e = 7.34 \times 10^{11} \text{ cm}^{-2}$ ;  $m_e = 0.0665 m_0$ ;  $d = 600 \text{ \AA}$ ;  $\omega_{ce}/\Omega_{pe} = 0.5, 0.9$ ;  $\epsilon_0 = 1.0$ .

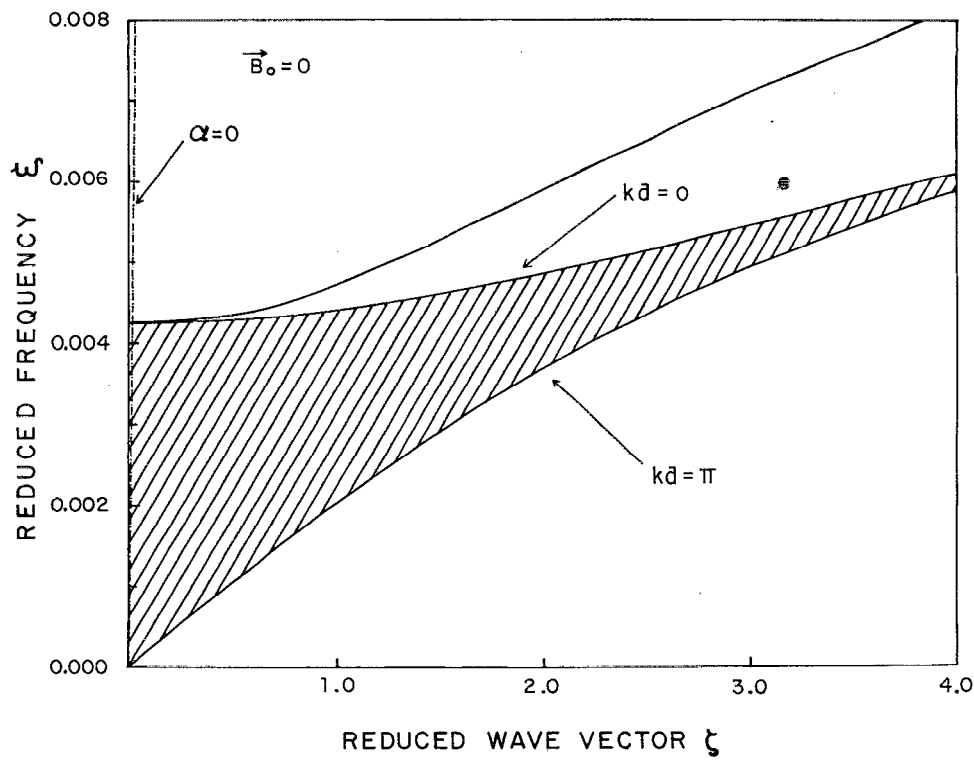


FIG. 2. Plasmon dispersion relation of type I superlattice plotted as  $\xi$  vs  $\zeta$  in the absence of an applied magnetic field. The shaded region is the band of the bulk intrasubband plasmons. The solid line is the surface polariton mode. The dash-dot line is the light line ( $\alpha=0$ ) in the background medium characterized by a dielectric constant  $\epsilon_s$ .

The case of the nonzero magnetic field is illustrated by the specific examples  $W_{ce} = \omega_{ce}/\Omega_{pe} = 0.5$  and  $0.9$  for which the results are shown, respectively, in Figs. 3 and 4. One immediately notes that the application of the magnetic field results in pushing the whole spectrum lying above  $\omega = \omega_{ce}$ . The shaded region is the bulk plasmon band whose lower edge, for  $k = \pi/d$ , starts at  $\omega \simeq \omega_{ce}$ . This can be seen by solving Eq. (15) in the strong coupling limit ( $\alpha d \ll 1$ ) to obtain

$$\omega = \omega_{ce} \left( 1 + \frac{1}{4} P^2 \right)^{-1} \simeq \omega_{ce}, \quad (21)$$

where  $P = (\Omega_{pe} d/c) \ll 1$ . The upper edge of the bulk band, for  $k=0$ , starts at a frequency given by

$$W^2 = \frac{1}{2} \left\{ \left( W_{ce}^2 + \frac{2}{\epsilon_s} \right) + \left[ \left( W_{ce}^2 + \frac{2}{\epsilon_s} \right)^2 - \frac{4}{\epsilon_s} \right]^{1/2} \right\}, \quad (22)$$

where  $W = \omega/\Omega_{pe}$  and  $W_{ce} = \omega_{ce}/\Omega_{pe}$ . In the limit of zero magnetic field (i.e.,  $W_{ce} = 0$ ), Eq. (22) reproduces the starting point of the  $k=0$  edge with  $\omega = \Omega_{pe}/\sqrt{\epsilon_s}$  (Fig. 2). The  $k=0$  mode starting at a frequency specified by Eq. (22) rises to the left of the light line  $\omega = cq/\sqrt{\epsilon_s}$  and becomes asymptotic to it. Another  $k=0$  mode is found to start at and remain to the right of the light line above the cyclotron frequency. This is the mode which merges with the  $k = \pi/d$  edge in the short wavelength limit and forms the bulk magnetoplasmon band in the long wavelength limit. What is interesting is to note that the  $k=0$  edge of

the bulk plasmon band in the presence of a transverse magnetic field observes a resonance splitting in the strong coupling limit. Such resonance splitting was also noted by Mizuno *et al.*<sup>15</sup> who used the quantum-mechanical conductivity tensor derived by Chiu and Quinn.<sup>16</sup> In the present treatment the resonance splitting can be justified by solving Eq. (15), for  $k=0$ , in the strong coupling limit. We obtain, neglecting the higher order corrections

$$q^2 \simeq q_0^2 \left[ \frac{1}{[1 - \epsilon_s(W^2 - W_{ce}^2)]} \left( \epsilon_s - \frac{1}{W^2} \right) + \epsilon_s \right]. \quad (23)$$

This reveals that although our perturbational approach breaks down (at  $W \simeq 1/\sqrt{\epsilon_s}$ ), it is clear that a resonance splitting occurs due to the interaction between the 2D magnetoplasma planes at

$$\omega_r^2 = \omega_{ce}^2 + \frac{1}{\epsilon_s} \Omega_{pe}^2. \quad (24)$$

It is noteworthy that such resonance splitting cannot be seen in the nonretarded limit where the  $k=0$  mode in the strong coupling limit is specified by a constant, effectively 3D magnetoplasmon frequency  $\omega_r$ . The resonance frequency  $\omega_r$  for the parameters used in the present computation corresponds to  $\xi \simeq 0.008749$  and  $0.014411$ , respectively, for  $W_{ce} = 0.5$  and  $0.9$ .

The magnetoplasma polariton mode starts at a frequency ( $\xi \simeq 0.00856$  and  $0.01429$ , respectively, for  $W_{ce} = 0.5$  and  $0.9$ ) just below the resonance frequency and

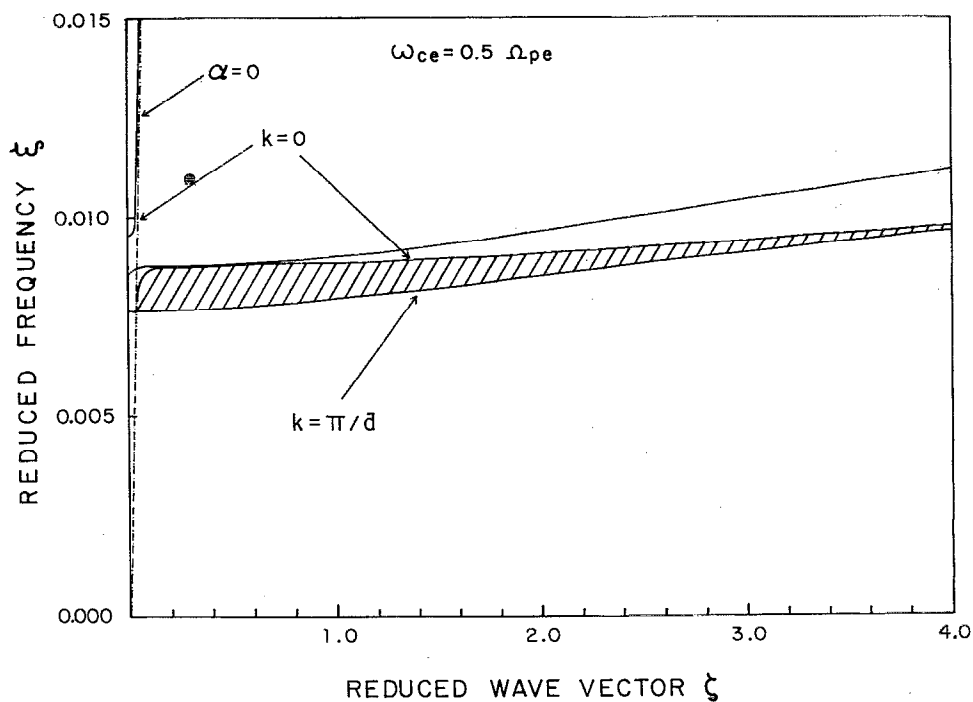


FIG. 3. Magnetoplasmon dispersion relation of type I superlattice in the presence of an applied magnetic field ( $\omega_{ce}=0.5 \Omega_{pe}$ ). The shaded region is the bulk magnetoplasmon band whose lower ( $k=\pi/d$ ) edge starts at  $\omega \approx \omega_{ce}$ . We call attention to the upper ( $k=0$ ) edge which observes a resonance splitting in the strong coupling limit. The solid line, towards the right of the light line ( $\alpha=0$ ), above the bulk band is the magnetoplasmon-polariton mode. The dotted part of the polariton mode, before intersecting the light line, refers to  $\alpha$  being imaginary.

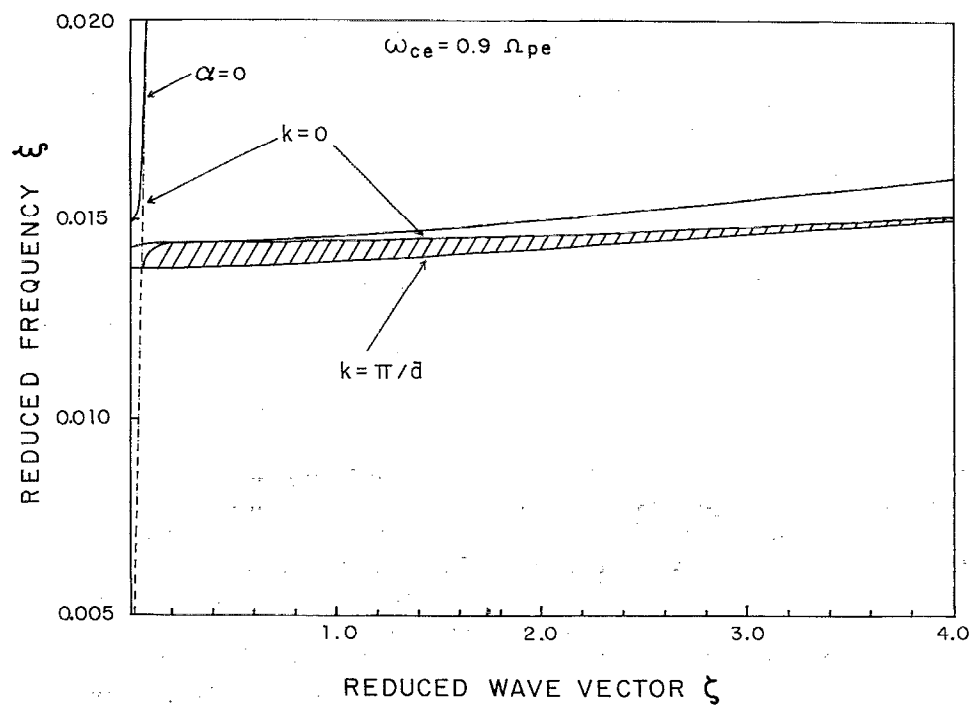


FIG. 4. Same as in Fig. 3 when the applied magnetic field is such that  $\omega_{ce}=0.9 \Omega_{pe}$ .



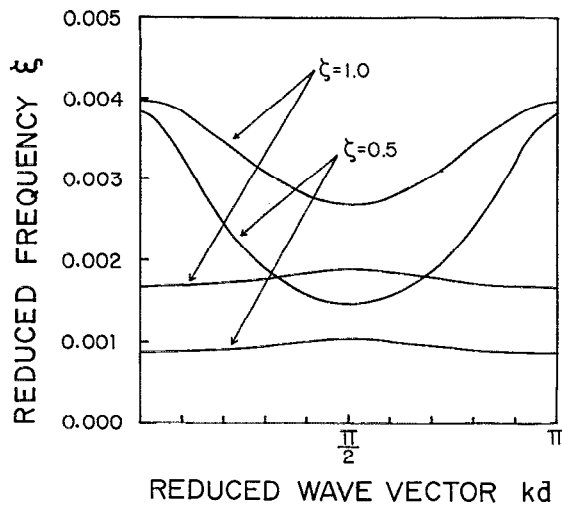


FIG. 5. Plasmon dispersion relation of type II superlattice plotted as  $\xi$  vs  $kd$ , for  $\zeta=0.5$  and  $1.0$ , in the absence of an applied magnetic field. The parameters used are:  $\epsilon_s=13.0$ ;  $n_e=n_h=4.2 \times 10^{11} \text{ cm}^{-2}$ ;  $m_e=2.0 m_h$ ;  $m_h=0.0665 m_0$ ;  $d=550 \text{ \AA}$ ;  $\omega_{ce}/\Omega_{pe}=0.5, 0.9$ ;  $\omega_{ch}/\Omega_{pe}=-(m_e/m_h) \times (\omega_{ce}/\Omega_{pe})$ . Here  $\Omega_{pi}=[4\pi n_e e^2/m_i(2d)]^{1/2}$  is the 3D unscreened plasma frequency;  $i=e,h$ .

becomes a bonafide mode (when  $\alpha$  is real and positive) after crossing the light line. In the long wavelength range ( $0.2 < qd < 0.5$ ), the polariton mode propagates in the close vicinity of the upper edge of the bulk band but it never merges into it. In the nonretarded limit, for large  $\zeta$ , Eq. (17) assumes a simple form

$$W^2 = \frac{1}{(\epsilon_s + \epsilon_0)}(qd) + W_{ce}^2. \quad (25)$$

Thus in this limit, the magnetoplasmon polariton is, in fact, the 2D magnetoplasmon supported by the 2DEG layer immersed in the two different dielectrics. We find that the polariton modes in Figs. 3 and 4 are exactly reproducible from Eq. (25), for  $\zeta > 3.0$ .

The effect of the magnitude of  $B_0$  on the plasmon dispersion and the resonance splitting can be seen by comparing the results depicted in Figs. 3 and 4. First we compare the magnitude of the splittings in the two cases. Measuring the vertical distances between the starting points of the two  $k=0$  edges of the bulk bands reveals that the resonance splitting ( $\Delta\xi$ ) decreases with an increasing magnetic field. With regard to the propagation characteristics, one immediately notes that the width of the bulk magnetoplasmon band decreases as the magnetic field increases. Also, the larger the magnetic field, the smaller is the separation of the polariton mode from the upper edge of the bulk band.

## B. Type II superlattice

We now turn to the numerical examples for bulk and surface excitations of the type II superlattice systems. Figure 5 shows the plot of  $\xi$  versus  $kd$  in the absence of the magnetic field. The broadening of the single 2DEG and 2DHG layer plasmons into the bands is evident. In analogy with the two masses per unit cell in the phonon dynamics,

the Brillouin zone is halved by the reduced periodicity producing one opticallike and the other acousticlike plasmon branches. This results in opening up a gap at the zone boundaries. The complete dispersion relations for bulk and surface plasmon polaritons in the absence of the magnetic field<sup>10</sup> are plotted in Fig. 6. The two shaded regions constitute the bulk plasmon bands whose boundaries occur at  $k=0$  and  $k=\pi/2d$ ,  $2d$  now being the superlattice period. At the zone center, the upper and the lower modes can be shown to start, respectively, at  $\omega=[(1+\Omega_r^2)/\epsilon_s]^{1/2}\Omega_{pe}$ , for  $k=0$ , and  $\omega=0$ , for  $k=\pi/2d$ . The variation of  $k$  from 0 to  $\pi/2d$  results in spatial separation between the two bulk bands provided the ratio  $\Omega_r(=\Omega_{ph}/\Omega_{pe})$  is different from unity. The two solid lines—one appearing above the upper edge of the upper bulk band and another occurring in the gap between the two bulk bands—are the surface plasmon polariton modes. Similarly to the corresponding case in type I superlattices, the features and location of the surface plasmon polaritons depend upon the ratio  $\epsilon_r=\epsilon_s/\epsilon_0$ .<sup>4,10</sup>

The upper polariton mode emerges from the upper edge of the upper bulk band at very short wave vectors and merges into it at large wave vectors. The critical wave vector  $q^*$  where this occurs also corresponds to the value of  $\alpha$  going to zero as the surface mode turns into a bulk mode. The value of  $q^*$  is found to be such that

$$\alpha d = \frac{1}{2} \ln \left| \frac{(1+\lambda)(1+\lambda\Omega_r^2)}{(1-\lambda)(1-\lambda\Omega_r^2)} \right|. \quad (26)$$

Equation (26), in the nonretarded limit, exactly reproduces Eq. (7) of Qin *et al.*<sup>5</sup> Again, we find that the inclusion of the retardation effects decreases the value of  $q^*$  and hence the limitation of ATR to observe this mode is ruled out. The lower polariton mode which appears within the gap between the two bulk plasmon bands never merges into either of the two bands. This is an acoustic surface plasmon polariton which, in the strong coupling limit ( $\alpha d \ll 1$ ), can be readily shown to satisfy the following dispersion relation

$$\omega \simeq \{2[\epsilon_s(1+\Omega_r^2)]^{-1}\}^{1/2}\Omega_{ph}(\alpha d) + 0(\alpha^2 d^2). \quad (27)$$

Equation (27) in the nonretarded limit, is exactly identical to Eq. (6) of Qin *et al.*,<sup>5</sup> with  $\omega \ll q$ . A novel feature of this acoustic mode is that it is free from Landau damping. That means that the collective mode has a long lifetime and hence represents a well-defined excitation of the system. The extensive investigations<sup>4-7</sup> on the collective excitations in the superlattice systems have, however, shown that this remarkable property (of being free from Landau damping) is a characteristic feature of the polariton modes of all types of superlattices and is attributed to the quantization of electronic motion along the superlattice axis.

We now focus on the numerical results for bulk and surface excitations of the 2D magnetoplasma in type II superlattice systems. The results are shown by the specific examples  $W_{ce}=0.5$  and  $0.9$ , respectively, in Figs. 7 and 8. We first discuss Fig. 7 and then compare the results with those presented in Fig. 8 in order to examine the effect of the intensity of the magnetic field. We find that when the magnetic field is switched on, the whole spectrum is

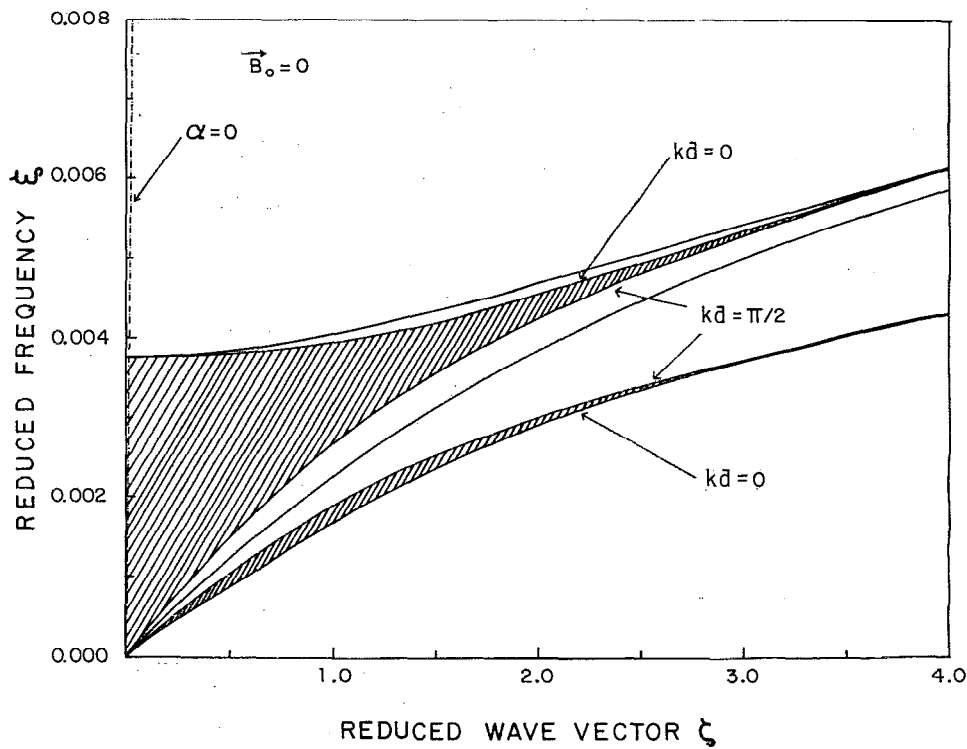


FIG. 6. Plasmon dispersion relation of type II superlattice plotted as  $\xi$  vs  $\zeta$  in the absence of an applied magnetic field. The two shaded regions are the bulk plasmon bands. The two solid line—one above the upper bulk band and another in the gap between the two bulk bands—are the surface polariton modes.

pushed to higher frequencies, lying above  $\omega = \omega_{ce}$  and the degeneracy between the two bulk bands (Fig. 6) is removed. The lower edges of the two bands (shaded regions) now start, for  $k = \pi/2d$ , at  $\omega = \omega_{ce}$  and  $\omega = \omega_{ch}$ , respectively. This can be seen by solving Eq. (8), for  $k = \pi/2d$ , in extreme long wavelength limit. The result is

$$\begin{aligned} & \{W^2[(1+P^2) + (1+\Omega_r^2 P^2) - 1] - W_{ce}W_{ch} \\ & + W[W_{ch}(1+P^2) - W_{ce}(1+\Omega_r^2 P^2)]\} \\ & \times \{W^2[(1+P^2) + (1+\Omega_r^2 P^2) - 1] - W_{ce}W_{ch} \\ & - W[W_{ch}(1+P^2) - W_{ce}(1+\Omega_r^2 P^2)]\} = 0, \end{aligned} \quad (28)$$

where  $W_{ce} = \omega_{ce}/\Omega_{pe}$ ,  $W_{ch} = \omega_{ch}/\Omega_{pe}$ , and the rest of the quantities are the same as defined earlier in the text. Now since  $\Omega_r$  is of the order of unity and  $P \ll 1$ , Eq. (28) reduces to

$$(W + W_{ch})(W + W_{ce})(W - W_{ce})(W - W_{ch}) = 0. \quad (29)$$

Either the third or the fourth factor is zero. As such Eq. (29) yields two modes:  $\omega = \omega_{ce}$  and  $\omega = \omega_{ch}$ . The upper edges of the two bulk bands, for  $k=0$ , which start from the zone center have almost the same story as the corresponding mode in the type I superlattice (Figs. 3 and 4). Their zone center frequencies are specified by

$$\begin{aligned} & \left[ W^2 + W(W_{ch} - W_{ce}) - \left[ W_{ch}W_{ce} + (1 + \Omega_r^2) \frac{1}{\epsilon_s} \right] \right] \\ & \times \left[ W^2 - W(W_{ch} - W_{ce}) - \left( W_{ch}W_{ce} + (1 + \Omega_r^2) \frac{1}{\epsilon_s} \right) \right] = 0 \end{aligned} \quad (30)$$

Here signs of  $W_{ch}$  and  $W_{ce}$  are both positive and  $\Omega_r^2 = W_{ch}/W_{ce}$ . Equating the first factor to zero yields

$$\begin{aligned} W &= \frac{1}{2} \left[ -W_{ce} + \left( 9W_{ce}^2 + \frac{12}{13} \right)^{1/2} \right] \\ &= \begin{cases} 0.640657 \Rightarrow \xi = 0.005020, & \text{for } W_{ce} = 0.5 \\ 0.982933 \Rightarrow \xi = 0.007703, & \text{for } W_{ce} = 0.9. \end{cases} \end{aligned} \quad (31)$$

Similarly, equating the second factor to zero gives

$$\begin{aligned} W &= \frac{1}{2} \left[ W_{ce} + \left( 9W_{ce}^2 + \frac{12}{13} \right)^{1/2} \right] \\ &= \begin{cases} 1.140657 \Rightarrow \xi = 0.008939, & \text{for } W_{ce} = 0.5 \\ 1.882933 \Rightarrow \xi = 0.014755, & \text{for } W_{ce} = 0.9. \end{cases} \end{aligned} \quad (32)$$

The upper mode (designated as  $U^+$ ) above the upper bulk band rises to the left of the light line and becomes asymptotic to it. The lower mode (designated as  $L^+$ ) also starts rising to the left of the light line but intersects the same ( $\alpha=0$ ) and bends down before approaching the lower edge of the upper bulk band to propagate to the right of the light

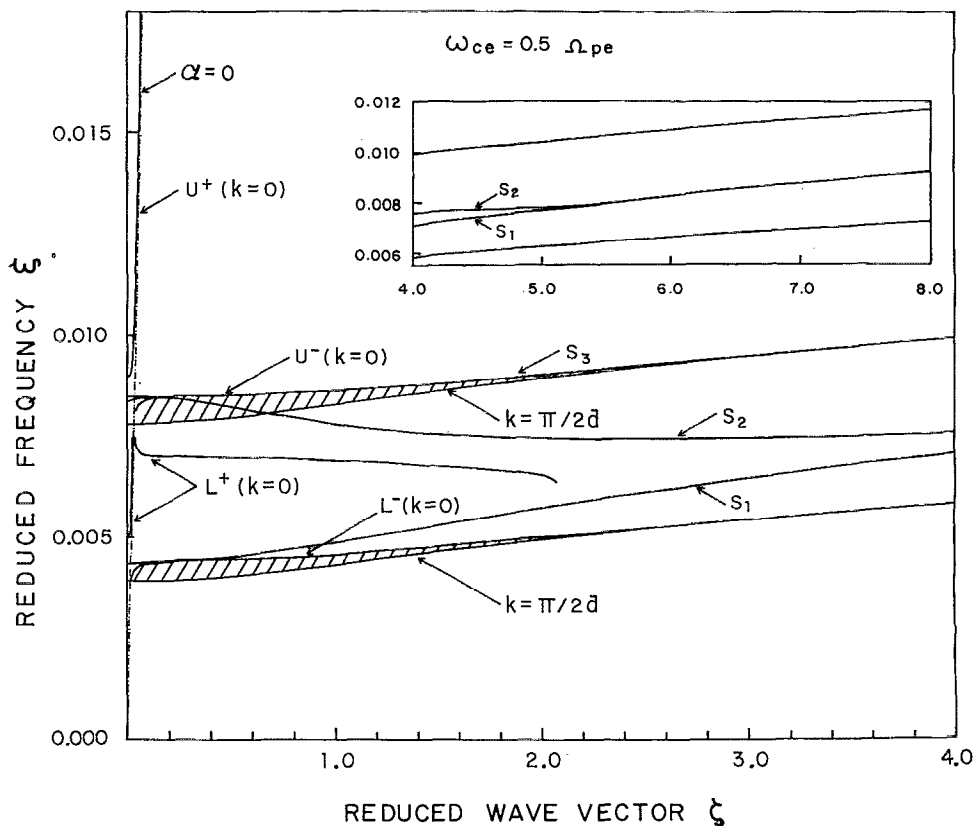


FIG. 7. Magnetoplasmon dispersion relation of type II superlattice in the presence of an applied magnetic field ( $\omega_{ce} = 0.5 \Omega_{pe}$ ). The two shaded regions are the bulk magnetoplasmon bands whose lower ( $k = \pi/2d$ ) edges start at  $\omega = \omega_{ce}$  and  $\omega = \omega_{ch}$ ;  $\omega_{ce}$  ( $\omega_{ch}$ ) being the electron (hole) cyclotron frequency. The upper ( $k=0$ ) edges of the two bulk bands display the resonance splittings in the strong coupling limit. The lower split modes ( $U^-$  and  $L^-$ ) start at the light line ( $\alpha=0$ ), just as in the case of type I superlattice (Figs. 3 and 4). The upper split mode above the upper bulk band ( $U^+$ ) becomes asymptotic to the light line, just as before (Figs. 3 and 4). The upper split mode in the gap ( $L^+$ ) intersects the light line before approaching the lower edge of the upper bulk band to propagate in the gap with a negative group velocity. This mode ( $L^+$ ), however, does not propagate at large  $\zeta$  ( $>2.07$ ). The solid lines, designated as  $S_1$ ,  $S_2$ , and  $S_3$ , represent the magnetoplasmon polariton modes. While  $S_3$  merges into the upper edge of the upper bulk band at very small  $\zeta$  ( $>0.14$ ),  $S_1$  and  $S_2$  propagate within the gap up to a considerably large  $\zeta$  before they merge together, but not with either of the bulk bands. This is shown in the inset.

line in the  $\omega-q$  space. However, it is found that this mode ( $L^+$ ) does not propagate for very large  $\zeta$  and stops at  $\zeta \approx 2.07$  (Fig. 7). The other  $k=0$  modes (designated as  $U^-$  and  $L^-$ ) are found to start at and propagate to the right of the light line above the respective cyclotron frequencies. These are the bonafide  $k=0$  modes which form the upper edges of the respective bulk bands. As such, we find that  $k=0$  edges of the bulk plasmon bands experience a resonance splitting in the presence of a transverse magnetic field. Such resonance splittings can be substantiated by solving Eq. (8), for  $k=0$ , in the strong coupling limit ( $\alpha d \ll 1$ ). We obtain, neglecting the higher order corrections,

$$q^2 [\epsilon_s (W^2 - W_{ce}^2) (W^2 - W_{ch}^2) - (W^2 - W_{ch}^2) - \Omega_r^2 (W^2 - W_{ce}^2)] \approx \left( \frac{q_0^2}{W^2} \right) [\epsilon_s (W + W_{ce})(W - W_{ch}) - (W - W_{ch})]$$

$$-\Omega_r^2 (W + W_{ce}) \times [\epsilon_s (W - W_{ce})(W + W_{ch}) - (W + W_{ch}) - \Omega_r^2 (W - W_{ce})]. \quad (33)$$

Again, the signs of  $W_{ch}$  and  $W_{ce}$  are decided to be positive. Although our perturbational approach breaks down (when either of the two factors on the right hand side of Eq. (33) vanishes), it is clear that a resonance splitting occurs due to interactions between 2D magnetoplasma planes at the frequencies which are the solutions of the biquadratic equation

$$W^4 - \left[ (W_{ce}^2 + W_{ch}^2) + \frac{1}{\epsilon_s} (1 + \Omega_r^2) \right] W^2 + [W_{ce}^2 W_{ch}^2 + \frac{1}{\epsilon_s} (\Omega_r^2 W_{ce}^2 + W_{ch}^2)] = 0. \quad (34)$$

It is worthwhile mentioning that such resonance splittings do not occur in the nonretarded limit where  $k=0$  modes in the strong coupling limit are the coupled 3D magneto-

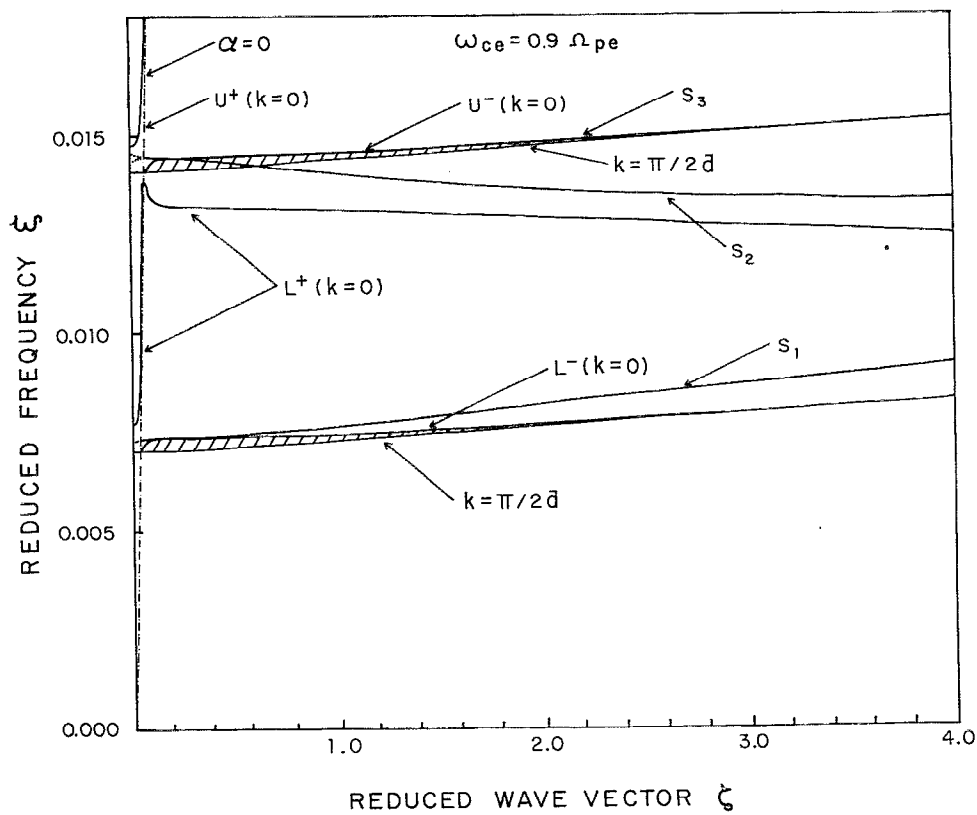


FIG. 8. Same as in Fig. 7 when the applied magnetic field is such that  $\omega_{ce} = 0.9 \Omega_{pe}$ . It is evident that the magnitude of the resonance splittings ( $\Delta\xi$ ) decreases with increasing magnetic field. On the other hand, the Zeemanlike splitting between the bulk bands and the polariton modes ( $S_1$  and  $S_2$ ) increases with the increasing magnetic field.

plasmons of a two-component (electron-hole) system. For the parameters used in the present computation, Eq. (34) is solved to obtain

$$\left. \begin{aligned} W_+ = 1.080703 &\Rightarrow \xi_+ = 0.008469 \\ W_- = 0.559331 &\Rightarrow \xi_- = 0.004903 \end{aligned} \right\}, \text{ for } W_{ce} = 0.5, \quad (35)$$

and

$$\left. \begin{aligned} W_+ = 1.843518 &\Rightarrow \xi_+ = 0.014447 \\ W_- = 0.939261 &\Rightarrow \xi_- = 0.007360 \end{aligned} \right\}, \text{ for } W_{ce} = 0.9, \quad (36)$$

where the subscripts  $+$  and  $-$  refer to the upper and the lower resonance splittings, respectively.

We now turn to the magnetoplasmon polariton modes of type II superlattice systems. In the presence of an external magnetic field, we find three polariton modes which are designated as  $S_1$ ,  $S_2$ , and  $S_3$  (Fig. 7). The lowest mode ( $S_1$ ) starts at  $\epsilon \approx 0.00434$  in the lower resonance region above the electron cyclotron frequency ( $\omega_{ce}$ ) with a positive group velocity. After the intersection with the light line (when  $\alpha = 0$ ), it extends in the very close vicinity of the upper edge of the lower bulk band ( $0.1 < \xi < 0.3$ ) and then propagates with increasing frequency towards large wave vectors within the gap. The second mode ( $S_2$ ) starts

at  $\epsilon \approx 0.00832$  in the upper resonance region above the hole cyclotron frequency ( $\omega_{ch}$ ) with a positive group velocity. When  $\alpha$  becomes real and positive, it extends to intersect (at  $\xi \approx 0.12$ ) with the upper edge of the upper bulk band to propagate with a negative group velocity until it reaches  $\xi \approx 2.02$ . At large wave vectors ( $\xi > 2.3$ ), it ( $S_2$ ) again assumes the positive group velocity (i.e., it propagates with frequencies increasing with the wave vectors). Thus we conclude that this is the polariton mode which changes the sign of its group velocity twice in the  $\omega - q$  space. The third polariton mode ( $S_3$ ) also starts in the upper resonance region at  $\xi \approx 0.00851$  with a negative group velocity and after intersecting the light line it propagates to merge with the upper edge of the upper bulk band. This leads us to infer that in the presence of an external magnetic field there are, practically, two magnetoplasmon polariton modes ( $S_1$  and  $S_2$ ) and both of them propagate within the gap between the two bulk bands. It is found that  $S_1$  and  $S_2$  modes also merge together at large wave vectors but they never merge with either of the bulk bands. This is shown in the inset in Fig. 7. It is not difficult to prove that the merger of  $S_1$  and  $S_2$  is quite likely at large  $\xi$ . We find that Eq. (12) in the nonretarded limit, for large  $\xi (=qd)$ , reduces to

$$(1 - \lambda)(1 + \frac{1}{2}C_1)(1 + \lambda + D_1) = 0. \quad (37)$$

The first factor does not vanish because  $\epsilon_s \neq \epsilon_0$ . The second factor equated to zero reproduces  $\omega^2 = \omega_{pe}^2 + \omega_{ch}^2$ , which is the well-known 2D bulk magnetoplasmon dispersion in the weak coupling limit.<sup>7</sup> Thus we are left with the only option that the last factor vanishes. This yields

$$W^2 = \frac{2}{(\epsilon_s + \epsilon_0)}(qd) + W_{ce}^2. \quad (38)$$

As such, we believe that the magnetoplasmon polaritons in the nonretarded (and weak coupling) limit, are effectively the magnetoplasmons supported by the 2DEG layer immersed in the two dielectrics characterized by the different dielectric constants  $\epsilon_s$  and  $\epsilon_0$ . It is interesting to note that Eq. (38) exactly reproduces the merger of  $S_1$  and  $S_2$  lying within the gap between the two bulk bands.

We compare the results on the magnetoplasmon dispersion relations plotted in Figs. 7 and 8 in order to examine the magnetic field effect. We find that the band widths decrease with the increasing magnetic field. The Zeeman splitting of the bulk bands increases as the magnetic field increases. The resonance splittings ( $\Delta\xi$ ) in the  $k=0$  edges of the bulk bands decrease, as compared to the respective splittings at lower  $B_0$  (Fig. 7), with the increasing magnetic field. We find, like the previous case (Fig. 7), three magnetoplasmon polaritons designated as  $S_1$ ,  $S_2$ , and  $S_3$ .  $S_1$  starts at  $\xi \simeq 0.00729$  in the lower resonance region above  $\omega_{ce}$ .  $S_2$  and  $S_3$  start, respectively, at  $\xi \simeq 0.01437$  and  $\xi \simeq 0.01457$  in the upper resonance region above  $\omega_{ch}$ . Their propagation characteristics are describable just as in the previous case (Fig. 7), except that  $S_1$  and  $S_2$  now merge at relatively larger  $\xi$ . Also the  $L^+$  ( $k=0$ ) mode stops propagating at considerably large  $\xi$  ( $\simeq 6.83$ ). It is found that the  $L^+$  mode does not interfere with  $S_1$  or  $S_2$  polariton modes and terminates before they merge together. Attempts to look for an analytical explanation for the termination of  $L^+$  ( $k=0$ ) mode at some  $\xi$  are thwarted by the mathematical complexity. We see that the smaller the magnetic field, the lower is  $\xi$  where  $S_1$  and  $S_2$  merge together.

## V. CONCLUSIONS

In this article we have provided a detailed theoretical investigation of the dispersion characteristics of 2D plasmons and magnetoplasmons in both type I and type II superlattice systems. The theoretical model is based on Maxwell's equations using a Dirac delta function for the charge density profiles. The most appealing feature of this theory is that the analytical results are readily conclusive to explain various critical propagation characteristics of magnetoplasmons in the  $\omega-q$  space. We have completely ignored the miniband structure of the superlattice systems

and consider only the ground subband and intrasubband collective excitations.

We conclude by pointing out that we have completely neglected the effects of carrier collisions. The effect of collisions on the damping of transverse modes, such as helicons, is known to be very important in 3D systems. Our neglect of collisions, however, can be justified by the fact that the superlattice systems are the highest mobility crystals in which the impurities are spatially well separated from the free charge carriers in the layers. Furthermore, experiments are generally performed at low temperatures where the scattering due to impurities (and disorder) can be very small. We have also neglected the coupling between the electronic collective excitations and the longitudinal optical (LO) phonons. In the systems in which the dielectric background is polarizable, as is the case in polar semiconductors, it is desirable to take into account the frequency dependence of  $\epsilon_s$ . A suitable way is to have  $\epsilon_s$  defined as  $\epsilon_s = \epsilon_\infty (\omega^2 - \omega_L^2) / (\omega^2 - \omega_T^2)$ , where  $\epsilon_\infty$  is the high frequency dielectric constant and  $\omega_L$  and  $\omega_T$  are, respectively, the longitudinal and transverse optical phonon frequencies at the center of the first Brillouin zone. The application of an external electric field, normal to the superlattice axis, which causes a relative drift in the current carriers and thereby produces an instability that leads to amplification is worth attention.

## ACKNOWLEDGMENTS

The author would like to thank Professor P. Halevi, Professor B. Djafari-Rouhani, and Professor L. Dobrzynski for many illuminating discussions. He also feels grateful to the Faculté des Sciences of Université de Haute Alsace (France) for their hospitality.

- <sup>1</sup>For the latest status of the field, see Proceedings of the Eighth International Conference on Electronic Properties of Two-Dimensional Systems. Surf. Sci. **229**, (1990).
- <sup>2</sup>S. Das Sarma and J. J. Quinn, Phys. Rev. B **25**, 7603 (1982); **27**, 6516 (E) (1983).
- <sup>3</sup>W. L. Bloss and E. M. Brody, Solid State Commun. **43**, 523 (1982).
- <sup>4</sup>G. F. Giuliani and J. J. Quinn, Phys. Rev. Lett. **51**, 919 (1983).
- <sup>5</sup>G. Qin, G. F. Giuliani, and J. J. Quinn, Phys. Rev. B **28**, 6144 (1983).
- <sup>6</sup>A. C. Tselis and J. J. Quinn, Phys. Rev. B **29**, 2021 (1984).
- <sup>7</sup>A. C. Tselis and J. J. Quinn, Phys. Rev. B **29**, 3318 (1984).
- <sup>8</sup>J. K. Jain and P. B. Allen, Phys. Rev. B **32**, 997 (1985).
- <sup>9</sup>R. D. King-Smith and J. C. Inkson, Phys. Rev. B **33**, 5489 (1986).
- <sup>10</sup>M. S. Kushwaha, J. Appl. Phys. **62**, 1895 (1987); **65**, 3303 (E) (1989).
- <sup>11</sup>J. K. Jain and S. Das Sarma, Surf. Sci. **196**, 466 (1988).
- <sup>12</sup>G. Eliasson, P. Hawrylak, Z. Zhu, X. Xia, and J. J. Quinn, Solid State Commun. **69**, 397 (1989).
- <sup>13</sup>U. Wulf, E. Zeeb, P. Gies, R. R. Gerhards, and W. Hanke, Phys. Rev. B **42**, 7637 (1990).
- <sup>14</sup>T. Ando, A. B. Fowler, and F. Stern, Rev. Mod. Phys. **54**, 437 (1982).
- <sup>15</sup>J. Mizuno, M. Kobayashi, and I. Yokota, J. Phys. Soc. Jpn. **39**, 983 (1975).
- <sup>16</sup>K. W. Chiu and J. J. Quinn, Phys. Rev. B **9**, 4724 (1974).